Design and Simulation of Torque Controller for Two-Mass Mechanical System Using Eigenvalue Analysis

Mansoor Zeinali[1,2], Somaye Yaghoubi[3,4*]

Abstract–Mechanical system in motor drive in industry can be modeled by multi-mass system. In this paper, the equations of the two-mass system are first stated in the state space and the two-mass mechanical system model is determined using the transfer functions. In torque control of this system, in order to have mechanical oscillation, PID controller is often used as a simple control method. Using the torque controller coefficients diagram method, it is designed and the behavior of the system is investigated and simulated using the analysis of eigenvalues. From the prominence of this study, we can mention the expression of electric torque changes in the two-mass system based on the inputs and their relationship with each other. The simulation results show that designing the parameters using the coefficient diagram method can reduce the fluctuations of the electric torque in the two-mass system. In this design, the eigenvalues of the system are placed on the left side of the imaginary axis.

Keywords: Two-mass mechanical system, Torque control, Transfer function, Eigenvalue analysis

1. Introduction

A mechanical system consisting of a number of masses such as motor, load and gear and connected to each other by a flexible shaft is called a multi-mass resonance system, which can be mentioned as examples of elevator system and steel rolling mill system [1-3].

The mechanical system in the industrial engine drive can be modeled by a multi-mass system [4-10].

In the motor moving system, if the motor and the load are connected by a fixed shaft, the movement of the motor system finds a mechanical oscillation, which is called a two-mass oscillating system [11,12]. The purpose of control in the two-mass oscillating system is to eliminate shaft rotation changes, return the load torque disturbance effect, quick response to base speed change without overshoot in load speed, and resistant stability [13,14].

Torsional fluctuations caused by rotor dynamics are one of the important topics in system dynamics. Torsional performance is a non-linear phenomenon, and the linear and mathematical model is a suitable tool system to investigate and diagnose and design against this phenomenon. The major problem of rotational oscillation in the flexible system arises when the load is connected to the motor through a long axis. Fluctuations are a major obstacle to increasing optimal system performance. The simplest model of this example of mechanical resonance systems is the two-mass system [15].

So far, various studies have been conducted in the field of multi-mass mechanical systems [16,17]. In [18], different methods for estimating the parameters of the two-mass mechanical system in electric drives are presented, in which a discrete-time output error model is applied to estimate the parameter, and the resulting pulse transfer function is converted into a continuous-time transfer function. and the parameters of the two-mass system model are solved analytically from the coefficients of this transfer function. The design of the model-based two-degree-of-freedom state space velocity controller for a two-mass mechanical system is proposed in [19], where the proposed design rules enable the automatic adjustment of the controller if the mechanical parameters are known. Also, the effects of time delay, measurement noise, and parameter changes on controller setting and control performance have been studied using Nyquist diagrams, noise transfer functions, and time domain simulations.

Various control methods for two-mass oscillating system such as nonlinear mode feedback control [20], resonance ratio control [21], neural network [22], robust control [23], slow resonance ratio control [24] and sliding mode control [25] has been presented so far.

1. Department of Electrical Engineering, Najafabad Branch, Islamic Azad University, Najafabad, Iran, Email: mansoor.zeinali@gmail.com
2. Smart Microgrid Research Center, Najafabad Branch, Islamic Azad University, Najafabad, Iran
3* Corresponding Author: Department of Mechanical Engineering, Najafabad Branch, Islamic Azad University, Najafabad, Irans, Email: yaghoubi@pmc.iaun.ac.ir
4. Modern Manufacturing Technologies Research Center, Najafabad Branch, Islamic Azad University, Najafabad, Iran
Received: 2022.09.23; Accepted: 2022.12.30

In this paper, the PID controller is used to control the torque in the two-mass mechanical system. To determine the controlling coefficients, the coefficient diagram method is used. The simulation results show the effect of the controller on the dynamic behavior of the system. The structure of the article is as follows. First, the equations of the two-mass system in the state space are stated in the second part, and the system model is determined using transfer functions in the Laplace domain. In the third part, the coefficients of the PID controller are determined. In the fourth part, the simulation results in Simulink MATLAB environment are presented. Finally, the conclusion is stated in the fifth part.

The highlights of this study include the following:

- Presentation of the two-mass resonance system model in the state space
- Displaying the system model based on transfer functions.
- Expression of electric torque changes in the system based on inputs and their relationship with each other.
- Controller design based on characteristic equation polynomial.
- Check changes in system response

2. Two-Mass Mechanical System Model

A simple structure of motor drive system with circulating load is shown in figure (1). The system consists of a drive motor and a load coupled to the motor through a shaft. If the stiffness of the shaft is low, the system will find mechanical oscillation. By choosing three state variables motor speed (ω_M), load speed (ω_L) and shaft torque (T_S) and two input variables motor torque (T_M) and load disturbance torque (T_L), the equations of state of the two-mass system in the circuit state Again, it is expressed in matrix form as follows [26,27]:

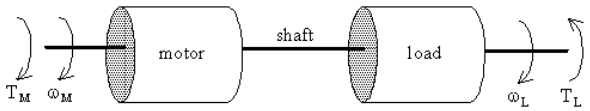

Fig. 1. Two-mass resonance system

$$\frac{d}{dt}X=\begin{bmatrix} -\frac{B_M}{J_M} & -\frac{1}{J_M} & 0 \\ K_S-\frac{B_M B_S}{J_M} & -B_S(\frac{1}{J_M}+\frac{1}{J_L}) & -(K_S-\frac{B_L B_S}{J_L}) \\ 0 & \frac{1}{J_L} & -\frac{B_L}{J_L} \end{bmatrix} X + \begin{bmatrix} \frac{1}{J_M} & 0 \\ \frac{B_S}{J_M} & \frac{B_S}{J_L} \\ 0 & -\frac{1}{J_L} \end{bmatrix} U \quad (1)$$

where J_L is load inertia, B_L is load damping coefficient, K_S is shaft stiffness coefficient, B_S is shaft damping coefficient, J_M is motor inertia, B_M is motor damping coefficient. The value of K_S depends on the material of the rotor and its shape. State variable vector and input vector are:

$$X=[\omega_M \quad T_S \quad \omega_L]^T \quad (2)$$

$$U=[T_M \quad T_L]^T \quad (3)$$

The block diagram of the two-mass resonance system can be shown according to Figure (2), where $G_L(s)$ is the load transfer function, $G_M(s)$ is the motor transfer function, and $G_S(s)$ is the shaft transfer function. As seen from the block diagram, we will have:

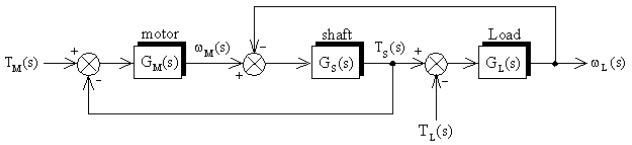

Figure (2): Block diagram of the resonance system of the two-mass system based on the transfer functions of the system components

$$T_S(s)=G_S(s)[\omega_M(s)-\omega_L(s)] \quad (4)$$

The shaft coupler consists of the sum of two signals, one of which is proportional to the difference in the speed of the motor and the load, and the other is proportional to the difference in the angles of the motor and the load, and due to the insignificant damping of the system, the torque of the shaft can be proportional to the difference in the angles of the motor and the load. Engine and load considered. The characteristic equation of the open circuit of the system is:

$$\Delta(s)=s^3+a_2 s^2+a_1 s+a_0 \quad (5)$$

The inertia ratio is equal to:

$$K_J=\frac{J_L}{J_M} \quad (6)$$

If the value of KJ is low, it is difficult to eliminate the torsional oscillations and more controller coefficients are needed. At KS=0, the characteristic equation has one root at the origin, and as the shaft stiffness coefficient increases, the roots move away from the imaginary axis. Shaft torque in terms of motor torque and load torque is equal to:

$$T_S(s)=\underbrace{\frac{G_M(s)G_S(s)}{1+G_M(s)G_S(s)+G_L(s)G_S(s)}}_{H_{SM}(s)}T_M(s)$$
$$+\underbrace{\frac{G_L(s)G_S(s)}{1+G_M(s)G_S(s)+G_L(s)G_S(s)}}_{H_{SL}(s)}T_L(s) \quad (7)$$

According to the roots of the quadratic equation, the resonant frequency and the damping coefficient are equal to:

$$\omega_R=\sqrt{a_1}=\sqrt{K_S\frac{J_M+J_L}{J_MJ_L}}=\sqrt{\frac{K_S}{J_L}(1+K_J)} \quad (8)$$

$$\eta=\frac{a_2}{2\omega_R}=\frac{B_S}{2}\sqrt{\frac{1}{K_SJ_L}(1+K_J)} \quad (9)$$

As can be seen, resonance frequency and damping coefficient are affected by inertia ratio (K_J). The value of B_S in most systems has a small value, and without BS, the damping value is zero [28,29]. The value of resonance frequency depends on the type of drive, and its value ranges from a few hertz in a printing machine, a few hundred hertz in a steel rolling machine, and a few thousand hertz in advanced servo drives.

3. Torque Controller Design

In this part, the method of coefficients diagram is explainned first, and then the system model for controller design using transfer functions is presented. Using this model, three proportional gain coefficients, integrator gain and derivative gain are determined for the controller.

3.1. Coefficient Diagram Method (CDM)

The coefficient diagram method is one of the algebraic methods that is developed based on the polynomial form and is considered between modern and traditional control theory. The design parameters in CDM are the stability index (γ_1) and the equivalent time constant (τ), which are defined based on the closed loop polynomial coefficients of the system. If the general form of the characteristic equation of the closed loop system with order n is considered as follows [30]:

$$\Delta(s)=a_ns^n+a_{n-1}s^{n-1}+.....+a_1s+a_0=\sum_{k=0}^{k=n}a_ks^k \quad (10)$$

The polynomial coefficients of the characteristic equation are expressed as follows [31]:

$$a_k=\frac{a_o\,\tau^k}{\gamma_{k-1}\gamma_{k-2}^2.....\gamma_1^{k-1}} \quad (11)$$

The ratio of two consecutive coefficients in a polynomial is equal to:

$$\frac{a_{k+1}}{a_k}=\frac{\tau}{\gamma_k\,\gamma_{k-1}\,\gamma_{k-1}.....\gamma_2\,\gamma_1} \quad (12)$$

The equivalent time constant determines the response speed and is considered based on the TS settling time as follows:

$$\tau=\frac{T_S}{2.5\sim3} \quad (13)$$

3.2. Torque Control System Model

PID controller is a simple and practical controller and for this reason it has been used in many systems [32-36].

Figure (3) shows the torque control block diagram for the two-mass oscillating system with PID controller. The transmission function of the shaft torque in terms of the desired torque specified in the input (T_C) and the load torque is:

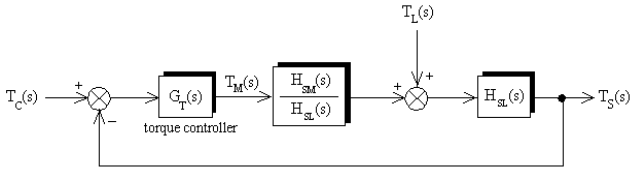

Fig. 3. Block diagram of torque control in two-mass resonance system

$$T_S(s)=H_{TC}(s)T_C(s)+H_{TL}(s)T_L(s) \quad (14)$$

Ignoring the damping coefficients of the system, the transfer function of the ratio of the shaft torque to the input torque is expressed as follows:

$$H_{TC}(s)=\frac{T_S(s)}{T_C(s)}=\frac{K_S\,K_{DT}\,s^2+K_S\,K_{PT}\,s+K_S\,K_{IT}}{J_M\,s^3+K_{DT}\,K_S\,s^2+(K_{PT}\,K_S+J_M\,\omega_R^2)s+K_{IT}\,K_S} \quad (15)$$

The frequency response of the system in closed loop mode is:

$$H_{TC}(j\omega)=\frac{\overbrace{K_S\,K_{IT}-K_S\,K_{DT}\,\omega^2}^{R_n(\omega)}+j\overbrace{K_S\,K_{PT}\,\omega}^{I_n(\omega)}}{\underbrace{K_{IT}\,K_S-K_{DT}\,K_S\,\omega^2}_{R_d(\omega)}+j\underbrace{\omega[K_{PT}\,K_S+J_M\,\omega_R^2-J_M\,\omega^2]}_{I_d(\omega)}} \quad (16)$$

As it can be seen, the real parts of Rn(ω) and Rd(ω) denominator are equal transfer function and in two frequencies ω_R and ω_G imaginary parts of In(ω) and Id(ω) denominator are equal transfer function. where the crossover frequency of the gain (the frequency at which the magnitude of the frequency response of the closed circuit equals one) is equal to:

$$\omega_G = \sqrt{\omega_R^2 + \frac{2K_S K_{PT}}{J_M}} = \omega_A \sqrt{1 + K_J (1 + 2K_{PT})} \qquad (17)$$

At frequencies ω_G and ω_R, the magnitude of the transfer function is equal to one and the phase of the transfer function has an effective change.

3.3. Torque Controller Design

In this part, the controller coefficients are determined according to the transmission function of the shaft torque to the desired torque. Based on the coefficients diagram method, the parameters τ, γ_1, γ_2 in the torque control closed-loop system in the two-mass resonant system, regardless of the system damping, are equal to:

$$\begin{cases} \tau = \dfrac{K_{PT} K_S + J_M \omega_R^2}{K_{IT} K_S} \\ \gamma_1 = \dfrac{(K_{PT} K_S + J_M \omega_R^2)^2}{K_{DT} K_S^2 K_{IT}} \\ \gamma_2 = \dfrac{K_{DT}^2 K_S^2}{J_M (K_{PT} K_S + J_M \omega_R^2)} \end{cases} \qquad (18)$$

Therefore, the coefficients of the PID controller are equal to:

$$\begin{cases} K_{PT} = \dfrac{J_M}{K_S}\left(\dfrac{\gamma_1^2 \gamma_2}{\tau^2} - \omega_R^2\right) = \dfrac{1}{K_J \omega_A^2}\left(\dfrac{\gamma_1^2 \gamma_2}{\tau^2} - \omega_R^2\right) \\ K_{IT} = \dfrac{J_M \gamma_1^2 \gamma_2}{K_S \tau^3} = \dfrac{\gamma_1^2 \gamma_2}{\tau^3 K_J \omega_A^2} \\ K_{DT} = \dfrac{J_M \gamma_1 \gamma_2}{K_S \tau} = \dfrac{\gamma_1 \gamma_2}{\tau K_J \omega_A^2} \end{cases} \qquad (19)$$

The time constant τ in terms of the crossover frequency of the gain is equal to:

$$\tau = \frac{\gamma_1 \sqrt{2\gamma_2}}{\sqrt{\omega_R^2 + \omega_G^2}} = \frac{\sqrt{2}}{\omega_R} \frac{\gamma_1 \sqrt{\gamma_2}}{\sqrt{1 + (\frac{\omega_G}{\omega_R})^2}} \qquad (20)$$

As can be seen, the value of τ is inversely proportional to ω_G and $\omega_G \geq \omega_R$ should be considered to reduce the vibration of shaft oscillations. Figure (4) shows the changes in controller gains in terms of the ratio of crossover frequency to their resonance frequency. This curve is independent of the parameters of the two-mass system and depends only on the stability index, which is selected as γ_1=2.5 and γ_2=2. The integral and proportional gains of the controller are more dependent on the resonance frequency than the crossover frequency, but the derivative gain changes of the controller are less.

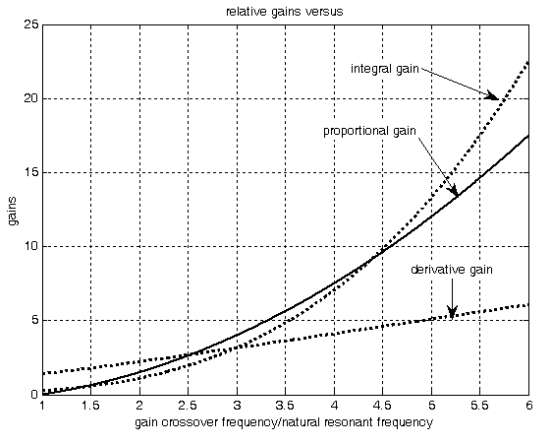

Fig. 4. Variations of the controller gains based on the ratio of the crossover frequency of the gain to the resonance frequency

4. Units Simulation Results

Figure (5) shows the model of the two-mass resonance system for shaft torque control with PID controller in Simulink environment. As can be seen, the torque of the shaft is compared with the desired torque and after passing through the controller, it forms the input torque of the motor. Considering that the characteristic equation of the two-mass resonance system with the controller is of the third order, therefore, only the stability indices γ_1 and γ_2 are considered. With the increase of the resonance coefficient and the inertia ratio, the time constant increases in proportion to the ratio of the cut-off frequency to the resonance frequency. Also, the increase of γ_1 and γ_2 decreases the integrator coefficient. The system parameters are selected according to table (1).

The eigenvalues of the system in the state without controller are: -1.2426 and -10.26±j137.14. As can be seen, in the state without controller, the characteristic equation has a negative real pole and two conjugate mixed poles, whose imaginary part is almost equal to the resonance frequency of the system. Figure (6) shows the frequency response of the transfer functions corresponding to the state variables in relation to the disturbance torque of the load and Figure (7) in relation to the motor torque, which shows the phase changes at the resonance frequency of 137.6 radians/second.

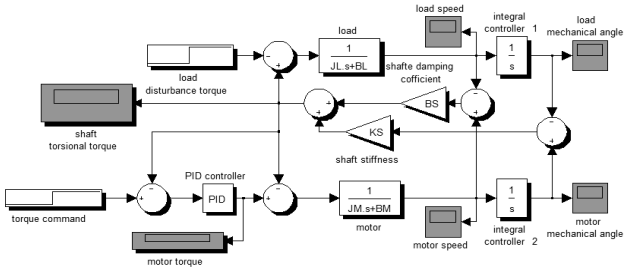

Fig. 5. Two-mass system model for shaft torque control with PID controller in Simulink environment

Table 1. Parameters of two-mass mechanical system

Symbol	Value
J_M	0.0480
B_M	0.0013
J_L	0.0086
B_L	0.0690
K_S	138
B_S	0.1
K_J	0.1792
ω_A	126.7
ω_R	137.6
K_R	1.09
η	0.0498
ω_L	53.6

The size of the transfer function corresponding to the motor speed at the anti-resonance frequency is 126.7 rad/s local minimum. In the load speed transfer function to the load disturbance couple, the transfer function has a local minimum at the frequency of 53.6 radians/s.

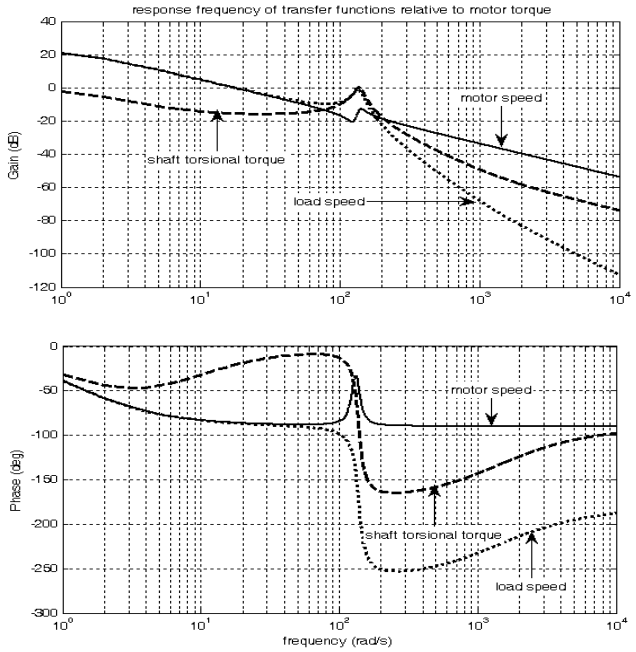

Fig. 6. Frequency response of transfer functions of motor speed, shaft torque and load speed in relation to motor torque

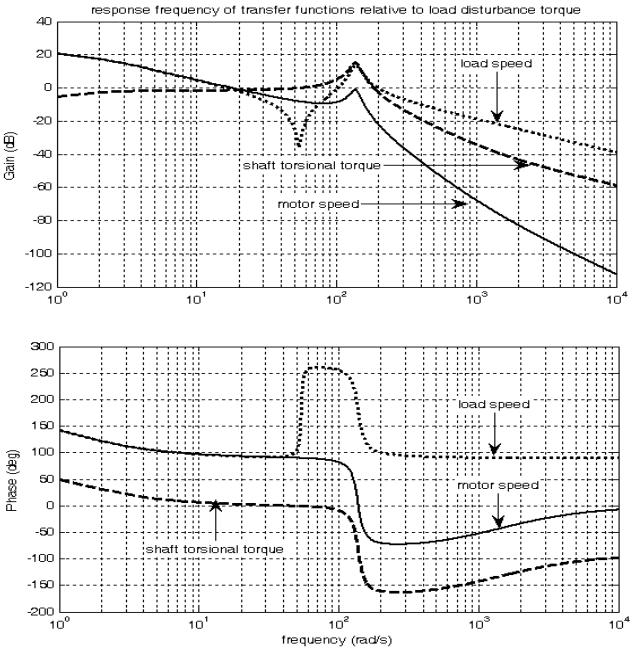

Fig. 7. Frequency response of transfer functions of motor speed, shaft torque and load speed in relation to the disturbance torque of the load

The frequency response of the transfer functions corresponding to the state variables relative to the two inputs of the motor coupler and the load disturbance coupler is shown in Figure (8), where the (--) response lines are relative to the motor coupler input and the (...) response lines are relative to The input is a load disturbance couple.

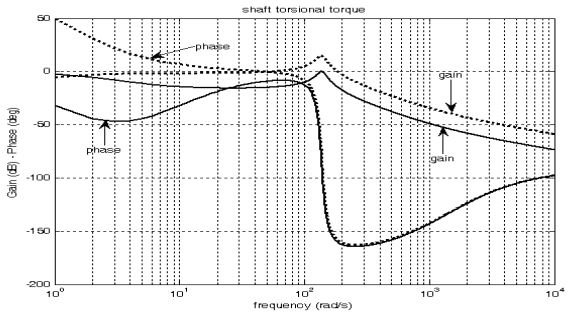

Fig. 8. Frequency response of the transfer function of the shaft torque to the motor torque and load disturbance torque

Table (2) shows controller gains and equivalent time constant for different values of cutoff frequency and two values of stability index.

Figure (9) shows the torque of the shaft and the torque of the motor with the PID controller for the three values determined in the table.

Figure (10) shows the geometric location of the roots of the characteristic equation of the closed loop system with torque control based on the changes of different parameters.

As can be seen from the geometric location of the roots, the system is stable for all values of proportional gain, but the condition of stability of integrator and derivative gain is expressed as follows:

$$K_D > \frac{J_M K_I}{K_P K_S + J_M \omega_R^2} \quad (21)$$

$$K_I < K_D(\omega_R^2 + \frac{K_P K_S}{J_M}) \quad (22)$$

Table 2. Controller gains in mode A for different cutoff frequency values

	γ_1=2.5, γ_2=2		
$\frac{\omega_G}{\omega_R}$	1	$\frac{3}{\sqrt{5}}$	3
K_{PT}	0	2.6326	26.3256
K_{IT}	256.0595	424.1632	2862.8
K_{DT}	0.0677	0.0801	0.1513
τ	0.0257	0.0217	0.0115

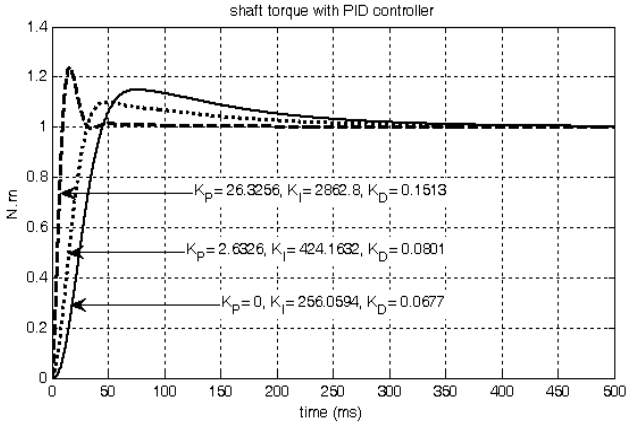

(a) coupling shaft

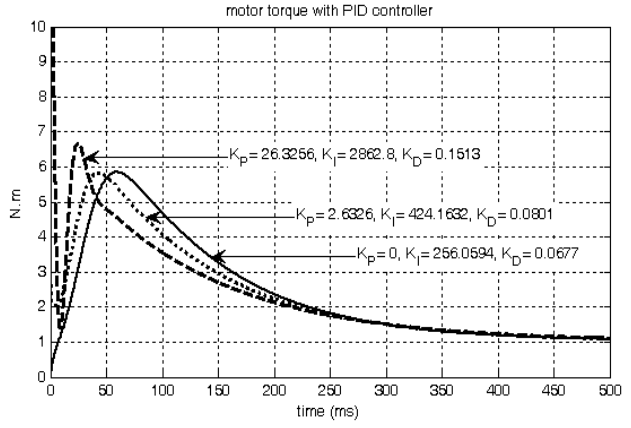

(b) engine coupler

Fig. 9. Response of shaft and motor couplings for different values of controller gain

Also, for the stability of the controller gain system, they should be selected so that the shaft torque coefficient applies in the following relationship:

$$K_S >< \frac{J_M K_I}{K_D K_P} - \frac{J_M \omega_R^2}{K_P} \quad (23)$$

A robust control keeps the closed loop system stable despite the uncertainties of the system. The closed loop system is stable if the Nyquist diagram does not go around the -1 point. If the controller is designed in such a way that not only does not bypass the -1 point, but also there is a large distance between the Nyquist diagram and this point, the Nyquist diagram can be slightly shifted despite not considering some nonlinear factors such as laxity in the model. and the closed loop system remains stable. Figure (3-33) shows the Nyquist diagram for two different values of K_D for parameters A, which is a stable system in one state and an unstable system in another state.

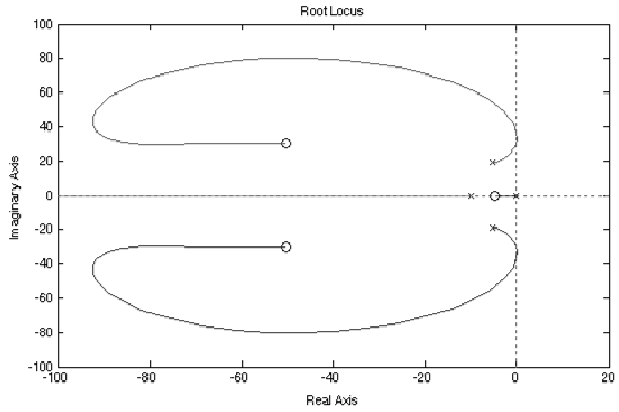

(a) Shaft stiffness factor

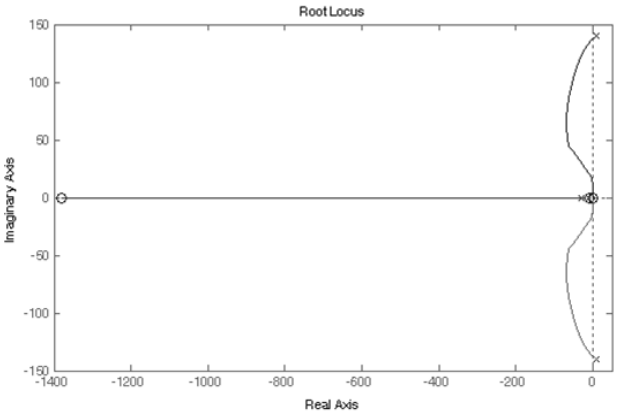

(b) The derivative coefficient of the controller

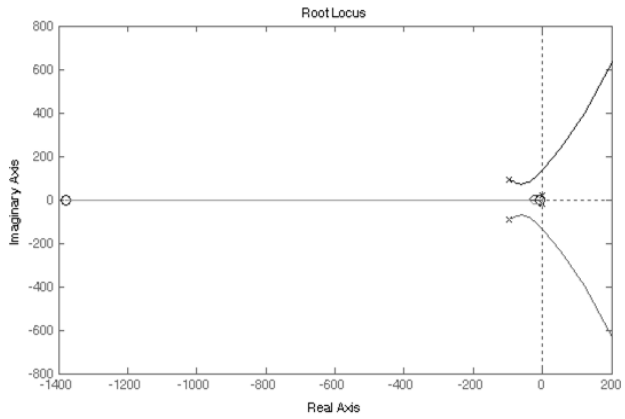

(c) the integrator coefficient of the controller

Fig. 10. The geometric location of the roots of the characteristic equation based on the changes of different parameters

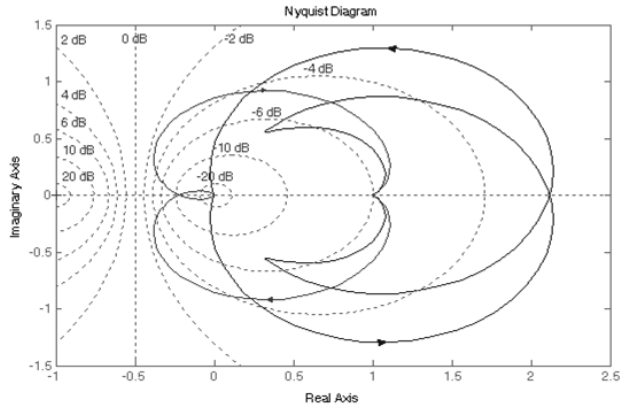

Fig. 11. Nyquist diagram for two different values of KD for stable and unstable system

5. Conclusion

In this design, a three-term controller is proposed using the coefficient diagram method to control the torque of the two-mass mechanical system. The use of this controller for torque damping was investigated using simulation results and eigenvalue analysis. Finally, the robustness of the controller was shown using the Nyquist diagram. To continue the research, other controller design methods such as the fuzzy method can be suggested.

References

[1] S. Brock, D. Łuczak, K. Nowopolski, T. Pajchrowski, K. Zawirski, "Two approaches to speed control for multi-mass system with variable mechanical parameters", IEEE Trans. on Industrial Electronics, vol. 64, no. 4, pp. 3338-3347, April 2017.

[2] G. Shahgholian, P. Shafaghi, M. Zinali, S. Moalem, "State space analysis and control design of two-mass resonant system", Proceeding of the IEEE/ICCEE, pp. 668-672, Dubai, Dec. 2009.

[3] T. Tezuka, T. Yamashita, T. Sato, Y. Abiko, T. Kanai, M. Sawada, "Application of a new automatic gauge control system for the tandem cold mill", IEEE Trans. on Industry Applications, vol. 38, no. 2, pp. 553-558, March/April 2002 .

[4] D. Luczak, T. Pajchrowski, "Application of adaptive neural controller and filter tune for multi-mass drive system", Proceeding of the IEEE/EPE, pp. 1-9, Riga, Latvia, Sept. 2018.

[5] A. Jafari, G. Shahgholian, "Analysis and simulation of a sliding mode controller for mechanical part of a doubly-fed induction generator based wind turbine", IET Generation, Transmission and Distribution, Vol. 11, No. 10, pp. 2677-2688, July 2017.

[6] F. Bendrat, C. Sourkounis, "Comparison of multi-mass models and modal models for state estimation of high power drives", Proceeding of the IEEE/EVER, pp. 1-7, Monte-Carlo, Monaco, May 2021.

[7] M.R. Yousefi, G. Shahgholian, A. Etesami, P. Shafaghi, "Small signal modeling and analysis of control speed for two mass resonant system", Proceeding of the IEEE/IPEC, pp. 1000-1003, Singapore, Oct. 2010.

[8] G. Shahgholian, "Modeling and simulation of a two-mass resonant system with speed controller", International Journal of Information and Electronics Engineering, vol. 3, no. 5, pp. 448-452, Sept. 2013.

[9] S. Lee, M. Kato, Y. Doi, K. Hirata, "A new method to control intrinsic localized mode using a variable magnetic spring structure", IEEE Trans. on Magnetics, vol. 58, no. 2, pp. 1-5, Feb. 2022.

[10] M. Fooladgar, E. Rok-Rok, B. Fani, G. Shahgholian, "Evaluation of the trajectory sensitivity analysis of the DFIG control parameters in response to changes in wind speed and the line impedance connection to the grid DFIG", Journal of Intelligent Procedures in Electrical Technology, Vol. 5, No. 20, pp. 37-54, March 2015 .

[11] J. Nandana, A.S. Anas, "An efficient speed control method for two mass drive systems using ADALINE", Proceeding of the IEEE/ICSTM, pp. 418-423 Avadi, India, May 2015.

[12] G. Shahgholian, "Controller design for three-mass resonant system based on polynomial method", International Journal of Science, Technology and Society, Vol. 5, No. 2, pp. 13-25, March 2017.

[13] K. Szabat, T. Tran-Van, M. Kamiński, "A modified fuzzy luenberger observer for a two-mass drive system", IEEE Trans. on Industrial Informatics, vol. 11, no. 2, pp. 531-539, April 2015.

[14] Y. Jin, C. Lu, P. Ju, C. Rehtanz, F. Wu, X. Pan, "Probabilistic preassessment method of parameter

identification accuracy with an application to identify the drive train parameters of DFIG", IEEE Trans. on Power Systems, vol. 35, no. 3, pp. 1769-1782, May 2020 .

[15] M. Taslimi, A. Chatraei, M. Hosseini, “A robust neuroadaptive control of three link SCARA robot with mass uncertainty”, Journal of Intelligent Procedures in Electrical Technology, vol. 4, no. 15, pp. 11-18, Nov. 2013 .

[16] G. Shahgholian, A. Hakimi, N. Behzadfar, ”Motor speed maximum control in the resonance ratio controller for two-mass system using self-organizing fuzzy controller”, International Journal of Research Studies in Electrical and Electronics Engineering, vol. 1, no. 6, pp. 1-8, 2020.

[17] P.K. Kundu, S. Chatterjee, “Nonlinear feedback self-excitation of modal oscillations in a class of under-actuated two degrees-of-freedom mechanical systems”, International Journal of Non-Linear Mechanics, vol. 135, Article Number: 103768, Oct. 2021 .

[18] S.E. Saarakkala, M. Hinkkanen, "Identification of two-mass mechanical systems using torque excitation: Design and experimental evaluation", IEEE Trans. on Industry Applications, vol. 51, no. 5, pp. 4180-4189, Sept./Oct. 2015 .

[19] S.E. Saarakkala, M. Hinkkanen, "State-space speed control of two-mass mechanical systems: Analytical tuning and experimental evaluation", IEEE Trans. on Industry Applications, vol. 50, no. 5, pp. 3428-3437, Sept./Oct. 2014 .

[20] E. Fuentes, D. Kalise, R.M. Kennel, "Smoothened quasi-time-optimal control for the torsional torque in a two-mass system", IEEE Trans. on Industrial Electronics, vol. 63, no. 6, pp. 3954-3963, June 2016.

[21] S. Katsura, K. Ohnishi, "Force servoing by flexible manipulator based on resonance ratio control", IEEE Trans. on Industrial Electronics, vol. 54, no. 1, pp. 539-547, Feb. 2007.

[22] A. Ilchmann, H. Schuster, "PI-funnel control for two mass systems", IEEE Trans. on Automatic Control, vol. 54, no. 4, pp. 918-923, April 2009.

[23] P. J. Serkies, K. Szabat, "Application of the MPC to the position control of the two-mass drive system", IEEE Trans. on Industrial Electronics, vol. 60, no. 9, pp. 3679-3688, Sept. 2013.

[24] Y. Hori, H. Sawada, Y. Chun, "Slow resonance ratio control for vibration suppression and disturbance rejection in torsional system", IEEE Trans. on Industrial Electronics, vol. 46, no. 1, pp. 162-168, Feb. 1999.

[25] T. Orlowska-Kowalska, M. Dybkowski, K. Szabat, "Adaptive sliding-mode neuro-fuzzy control of the two-mass induction motor drive without mechanical sensors", IEEE Trans. on Industrial Electronics, vol. 57, no. 2, pp. 553-564, Feb. 2010.

[26] G. Shahgholian, J. Faiz, P. Shafaghi, "Analysis and simulation of speed control for two-mass resonant system", Proceeding of the IEEE/ICCEE, pp. 668-672, Dubai, Dec. 2009.

[27] G. Shahgholian, J. Faiz, "An analytical approach to synthesis and modeling of torque control strategy for two-mass resonant systems", International Review of Automatic Control, Vol. 2, No. 4, pp. 459-468 , July 2009.

[28] K. Szabat, T. Orlowska-Kowalska, "Optimization of the two-mass drive dynamics using different compensation feedbacks", Proceeding of the IEEE/OPTIM, pp. 19-24, Brasov, Romania , May 2008.

[29] G. Ellis, R.D. Lorenz, "Resonant load control methods for industrial servo drives", Proceeding of the IEEE/IAS, vol. 3, pp. 1438-1445, Rome, Italy , Oct. 2000.

[30] Y. Nakayama, K. Fujikawa, H. Kobayashi, "A torque control method of three-inertia torsional system with backlash", Proceeding of the IEEE/AMC, pp. 193-198, Nagoya, Japan, April 2000.

[31] M. Odai, Y. Hori, "Speed control of 2-inertia system with gear backlash using gear torque compensator", Proceeding of the IEEE/AMC, pp. 234-239, Coimbra, Portugal, June/July 1998.

[32] M. Lotfi-Forushani, B. Karimi, G. Shahgholian, “Optimal PID controller tuning for multivariable aircraft longitudinal autopilot based on particle swarm optimization algorithm”, Journal of Intelligent Procedures in Electrical Technology, vol. 3, no. 9, pp. 41-50, June 2012.

[33] N. Taheri, H. Orojlo, F. Ebrahimi, "Damping controller design in offshore wind power plants to improve power system stability using fractional order PID controllers based on optimized exchange market algorithm", Journal of Intelligent Procedures in Electrical Technology, vol. 13, no. 51, pp. 91-110, Dec. 2022.

[34] R. Shahedi, K. Sabahi, M. Tayana, A. Hajizadeh, “Self-tuning fuzzy PID controller for load frequency control in ac micro-grid with considering of input

delay", Journal of Intelligent Procedures in Electrical Technology, vol. 9, no. 35, pp. 19-26, Dec. 2019.

[35] G. Shahgholian, A. Etesami, M. R. Yousefi, F.M. Tehrani, "Development of state space model and control design of two-mass system using standard forms", Proceeding of the IEEE/ICCSN, pp. 342-346, Xi'an, China, May 2011.

[36] M. Jeddi-Golfazani, M. Vahedi, M. Gandomkar, "Design of robust reset controller based on optimal after reset performance to improve the performance of an industrial robot control", Journal of Intelligent Procedures in Electrical Technology, vol. 14, no. 55, pp. 83-100, Dec. 2023.